Platinum-Group Mineral Occurrences and Platinum-Group Elemental Geochemistry of the Xiadong Alaskan-Type Complex in the Southern Central Asian Orogenic Belt

Sai-Hong Yang [1,2,*], **Ben-Xun Su** [2,3], **Xiao-Wen Huang** [4], **Dong-Mei Tang** [2], **Ke-Zhang Qin** [2,3], **Yang Bai** [2,3], **Patrick Asamoah Sakyi** [5,*] **and Melesse Alemayehu** [1,6]

[1] State Key Laboratory of Lithospheric Evolution, Institute of Geology and Geophysics, Chinese Academy of Sciences, P.O. Box 9825, Beijing 100029, China; melesse555@yahoo.com

[2] Key Laboratory of Mineral Resources, Institute of Geology and Geophysics, Chinese Academy of Sciences, Beijing 100029, China; subenxun@mail.iggcas.ac.cn (B.-X.S.); tdm@mail.iggcas.ac.cn(D.-M.T.); kzq@mail.iggcas.ac.cn (K.-Z.Q.); by@mail.iggcas.ac.cn (Y.B.)

[3] University of Chinese Academy of Sciences, Beijing 100049, China

[4] State Key Laboratory of Ore Deposit Geochemistry, Institute of Geochemistry, Chinese Academy of Sciences, Guiyang 550081, China; huangxiaowen@vip.gyig.ac.cn

[5] Department of Earth Science, University of Ghana, P.O. Box LG 58, Legon-Accra 00233, Ghana

[6] School of Applied Natural Science, Department of Applied Geology, Adama Science and Technology University, P.O. Box 1888, Adama 00251, Ethiopia

* Correspondence: shyang@mail.iggcas.ac.cn (S.-H.Y.); pasakyi@ug.edu.gh (P.A.S.);
  Tel.: +86-010-8299-8592 (S.-H.Y.); Fax: +86-010-62010846 (S.-H.Y.)

Abstract: Alaskan-type complexes commonly contain primary platinum-group element (PGE) alloys and lack base-metal sulfides in their dunite and chromite-bearing rocks. They could therefore host PGE deposits with rare sulfide mineralization. A detailed scanning electron microscope investigation on dunites from the Xiadong Alaskan-type complex in the southern Central Asian Orogenic Belt revealed: various occurrences of platinum-group minerals (PGMs) that are dominated by inclusions in chromite grains containing abundant Ru, Os, S and a small amount of Pd and Te, indicating that they mainly formed prior to or simultaneously with the crystallization of the host minerals; A few Os–Ir–Rurich phases with iridium/platinum-group element (IPGE) alloy, anduoite $(Ru,Ir,Ni)(As,S)_{2-x}$ and irarsite (IrAsS) were observed in chromite fractures, and as laurite (RuS_2) in clinopyroxene, which was likely related to late-stage hydrothermal alteration. The rocks in the Xiadong complex display large PGE variations with ∑PGE of 0.38–112 ppb. The dunite has the highest PGE concentrations (8.69–112 ppb), which is consistent with the presence of PGMs. Hornblende clinopyroxenite, hornblendite and hornblende gabbro were all depleted in PGEs, indicating that PGMs were likely already present at an early phase of magma and were mostly collected afterward in dunites during magma differentiation. Compared with the regional mafic–ultramafic intrusions in Eastern Tianshan, the Xiadong complex show overall higher average PGE concentration. This is consistent with the positive PGE anomalies revealed by regional geochemical surveys. The Xiadong complex, therefore, has potential for PGE exploration.

Keywords: Alaskan-type complex; Central Asian Orogenic Belt; PGM; PGE mineralization

1. Introduction

Platinum-group element (PGE) mineralization in Alaskan-type complexes is invariably present in dunite units [1,2], occasionally in the vein-type settings associated with bodies of magnetite-rich clinopyroxenite in the dunite or peridotite core, in pegmatitic and micaceous rocks [3]. Previous studies revealed general enrichments in Pt, Pd and Rh relative to Ru, Ir and Os in Alaskan-type complexes [4,5]. Platinum-rich minerals, mainly Pt–Fe alloys are thought to form in the early stages of magmatic evolution and are associated with chromite formation [6]. Palladium-rich minerals on the other hand form at later stages and are associated with Cu–Fe–V–Ti metal formation [4,7]. As the Alaskan-type complexes originated from highly oxidizing and low-sulfur magmatism [8], they commonly occur with the presence of PGE alloys and lack base-metal sulfides [8]. However, sulfide mineralization coupled with chromite and/or PGE mineralization was explored in a few Alaskan-type complexes (e.g., Turnagain, British Columbia; and Duke Island, Alaska) [9,10]. This discrepancy is not well understood. Further investigation into the occurrences and geochemical histories of chromites, platinium-group minerals (PGMs) and sulfides is required in these Alaskan-type complexes.

Geological survey mapping of ultralow density using chemical spectrometry analysis of Pt, Pd and Au from floodplain overbank sediment samples revealed PGE anomalies in the Eastern Tianshan orogen for a long time [11]. Platinum-group element deposits are yet to be found in this area, although an increasing number of Ni–Cu sulfide deposits were identified in Permian mafic–ultramafic intrusions [12–14]. The Xiadong mafic–ultramafic complex in the Mid-Tianshan Terrane, the southern part of the Eastern Tianshan orogen, differs from the Ni–Cu sulfide deposit-hosting mafic–ultramafic intrusions in terms of its geochronology, petrology, mineralogy and geochemistry [15–20]. It is composed of dunite, hornblende clinopyroxenite, hornblendite and hornblende gabbro. These rocks are characterized by cumulate textures, high Mg contents, low trace–element abundances, flat rare-earth element (REE) and arc-magma-type trace-element patterns, and considerable Mg isotopic variations at both mineral and whole-rock scales [15,17–20]. The Xiadong complex was formed following multiple magmatic pulses according to zircon U–Pb ages (479, 477, 379, and 313 Ma) of four hornblende gabbros [17]. It was been identified as a typical Alaskan-type complex showing potential chromite mineralization [15]. A more recent study reported the discovery of base-metal minerals in ultramafic rocks of the Xiadong Alaskan-type complex [18]. In order to investigate potential PGE and metal sulfide mineralization in the Xiadong complex, we present the observations of PGMs and sulfides as well as PGE whole-rock geochemistry of Xiadong intrusive rocks. The Xiadong complex shows variable but relatively higher PGE concentrations when compared with regional mafic–ultramafic intrusions. The complex, thus, has potential for PGE exploration. The PGM and sulfide segregations in this Alaskan-type complex are also discussed.

2. Geological Background

The Eastern Tianshan and Beishan orogens are located in the southern part of the Central Asian Orogenic Belt (CAOB) (Figure 1A). Numerous mafic–ultramafic intrusions are widespread in the orogens and they host the major Ni–Cu sulfide deposits in China [14,21,22] (Figure 1B). These mafic–ultramafic intrusions formed mostly at the post-orogenic extensional setting in the early Permian [12–15]. Results of geochemical exploration revealed that the positive PGE anomalies (0.4–0.6 ppb Pt and 0.4–1.0 ppb Pd) are spatially related with the mafic–ultramafic intrusions in the Eastern Tianshan and Beishan [11,23]. However, progress is yet to be made on PGE deposit exploration in this area.
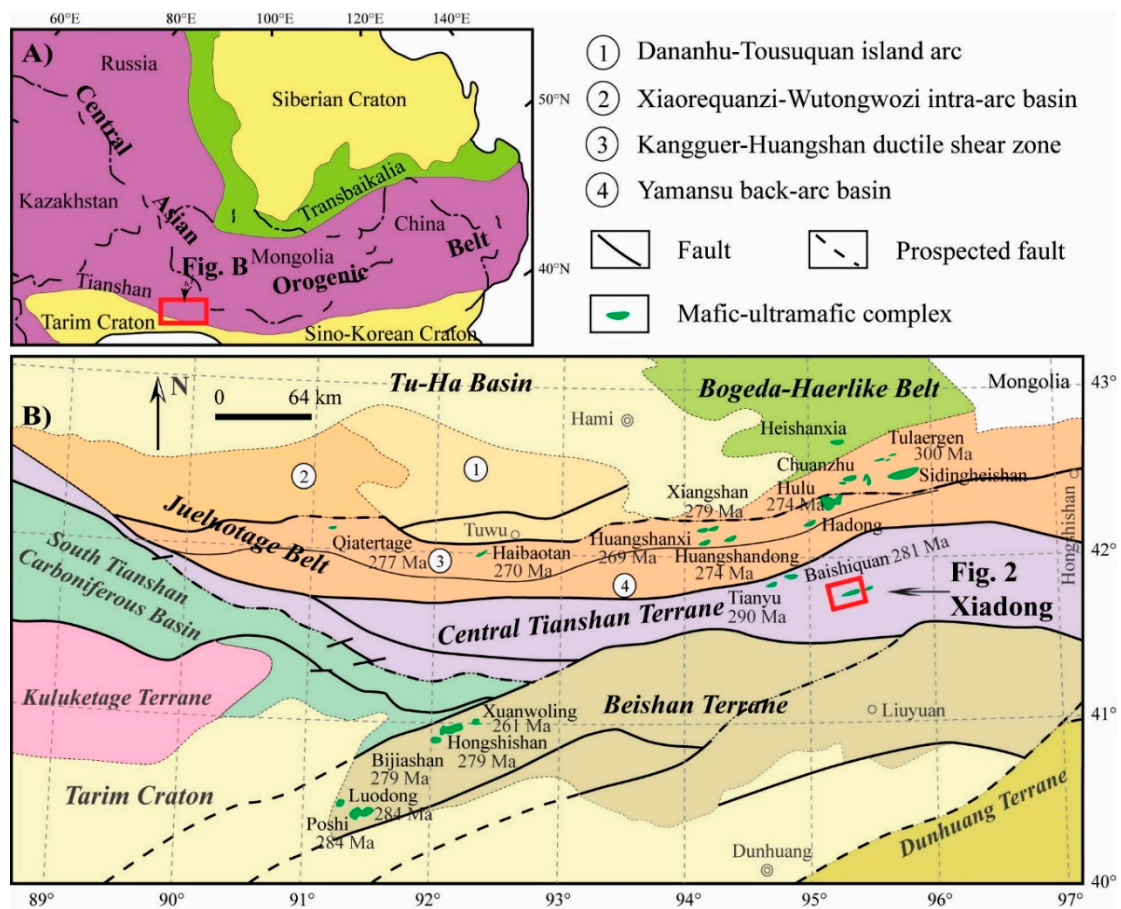
Figure 1. (**A**) Location map of the study area in the Central Asian Orogenic Belt. (**B**) Geological map of the Eastern Tianshan and Beishan orogens showing the distribution of Paleozoic mafic–ultramafic complexes (modified from References [15,17]). The reported numbers represent the ages of known intrusions.

The Xiadong mafic–ultramafic complex is situated in the Mid-Tianshan Terrane (Figure 1B), which is interpreted as a continental arc from the Ordovician to the Carboniferous. The complex was formed by multiple pulses of magma via high-degree melting of the lithospheric mantle, most likely related to subduction of the South Tianshan ocean and subsequent subduction of the Junggar ocean. The detailed geology was summarized by Tang et al. and Su et al. [17,24]. The Xiadong complex stretches east–west and covers an area measuring 7 km in length with a maximum width of 0.5 km. It has distinctive petrological and mineralogical features relative to the Permian mafic–ultramafic intrusions in Eastern Tianshan and Beishan. The Xiadong complex is composed of dunite in the core and surrounded by hornblende clinopyroxenite, hornblendite and hornblende gabbro (Figure 2), representing a complete set of rock suites compared with other Alaskan-type complexes worldwide [15,18]. These rock units are characterized by cumulate textures and display intrusive contacts with the country rocks [15].
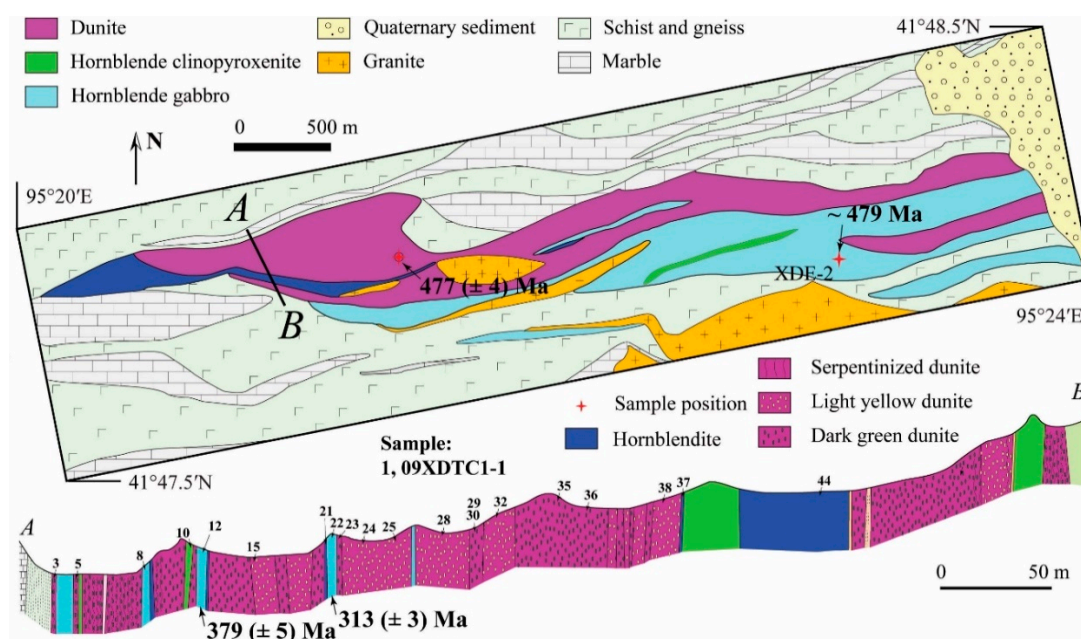
Figure 2. Geological map of the Xiadong mafic–ultramafic complex, accompanied by a horizontal profile along A to B showing its rock units and sampling positions (modified from References [15,17]). Isotopic ages are the U–Pb ages of zircons from four hornblende gabbros.

3. Materials and Analytical Methods

3.1. Sample Description

The studied rocks were mostly fresh with slight alteration. The minerals in the complex are dominated by olivine, clinopyroxene, and hornblende with accessory chromite and magnetite. Orthopyroxene is very rare in all of the rock units. Plagioclase is absent in the dunite and hornblende clinopyroxenite. The dunite is made up of olivine (90–98 vol.%) and chromite (0.5–8 vol.%) with accessory hornblende and clinopyroxene (<1–2 vol.%). The Fo content of olivine in the dunites ranges from 92 to 96.7 [15,18]. Subhedral to euhedral interstitial chromite occurs in elongated crystal or rounded shapes.

3.2. Sample Preparation

Samples were collected using a hammer before polishing thin sections for optical microscopy work. From the samples, 14 polished thin sections including eight dunite samples, two hornblende clinopyroxenite samples, two hornblendite samples, and two hornblende gabbro samples were prepared for electron microscopy work. The thin sections were then coated with the carbon with ~10 nm thickness using a Leica EM ACE200 coating equipment (Leica, Vienna, Austria). Sixteen samples extracted from the different rock units were also crushed into powder with 200 mesh for measuring PGE concentrations.

3.3. Sample Analyses

The thin sections were studied using a FEI Nova Nano450 scanning electron microscope (SEM) equipped with an energy dispersive X-ray spectrometer (EDS) from Oxford Instruments (High Wycombe, UK) at the Institute of Geology and Geophysics, Chinese Academy of Sciences. Backscattered electron (BSE) images were obtained at an accelerating voltage of 10 kV and a beam current of 3.0 nA. The acquisition time of one BSE image was ~1 min. Semi-quantitative spot analyses and EDS mapping were obtained at an accelerating voltage of 20 kV and a beam current of 8.8 nA.

The acquisition time of each spot was about 15 s, ensuring the spectrum area exceeded 2.5×10^6 counts. The mapping determination of each grain took about 5 min, with a dwell time of 5 μs for each pixel.

Whole-rock PGE concentrations were measured at the State Key Laboratory of Ore Deposit Geochemistry, Institute of Geochemistry, Chinese Academy of Sciences. The concentrations were determined by isotope dilution (ID) inductively coupled plasma (ICP)-MS using a modified digestion method [25,26]. Five grams of rock powder (>200 mesh) and appropriate amounts of ^{101}Ru, ^{193}Ir, ^{105}Pd and ^{194}Pt isotope spikes were used. The PGE measurements were made with a Perkin Elmer Elan DRC-e ICP-MS. Ir, Ru, Pt and Pd concentrations were measured by isotope dilution, and Rh concentrations were calculated using ^{194}Pt as an internal standard [27]. The analyses were monitored using the standard reference materials, WGB-1 (gabbro) and TDB-1 (diabase). Measured values were in good agreement with certified values. The total procedural blanks were lower than 0.009 ng for Ru, Rh, and Ir, and 0.030 ng for Pt and Pd.

4. Results

4.1. Occurrences of PGM and Sulfide

Fourteen samples were investigated using SEM. PGMs were only found in dunite sample. The number of identified grains per sample was different. There were about nineteen grains with sizes of less than one micron, as well as two grains of about four microns, from eight dunite samples. Limited by the resolution of SEM, some micro-scale individual grains with PGE elements detected by EDS could not be imaged. Some of the back scattered electron images and EDS analyses are shown in Figures 3–7 and Table 1.

Platinum-group minerals mostly occur as inclusions in chromite from sub-micrometer to several tens of nanometers in size (Figures 3–5 and Figure 6a). These PGM inclusions are composed of PGE sulfides and tellurides, dominated by Os–Ru–S with seven grains discovered in five samples (Figure 3a–c), Ru–S with six grains discovered in five samples (Figure 3d) and Os–Ru–Pd–Te with three grains discovered in two samples (Figure 3e,f).

Two PGMs were observed in fractures of chromite in one sample. One grain was only about ten nanometers in size, appearing irregular in shape. The larger grain forming composite grain with a maximum diameter of 4×3 microns, displays a well-defined contact with chromite (Figure 4a). The BSE image and EDX maps in Figure 4 show that the Ir and Pt distributions positively correlate with S in the grain, whilst Ru and Ni positively correlate with As distribution (Figure 4c–i). The average composition measured by EDS on the basis of a total of 3 number of atoms in one molecule or formula unit (apfu). gave $(Ru_{0.89}Ir_{0.27}Ni_{0.10}Pt_{0.08})\Sigma_{1.3}(As_{1.36}S_{0.30})\Sigma_{1.7}$ (Table 1) and $Ir_{0.77}Ru_{0.08}As_{0.76}S$, corresponding to the formula $(Ru,Ir,Ni)(As,S)_{2-x}$ likely to be anduoite [28] and IrAsS, known as irarsite, respectively. Osmium was concentrated in a local area (Figure 4c), measuring 52.9 wt.% Os, 11.6 wt.% Ir and 34.5 wt.% Ru (Table 1), indicating that it was an alloy.

An elliptical grain of laurite (about 5 μm in size) was observed in clinopyroxene (Figure 5). This grain contained S, Ru, and Se with small amounts of Os, Ir, and Ni. The average composition of the laurite from EDS was $Ru_{0.47}Fe_{0.09}Os_{0.03}Ir_{0.03}Ni_{0.02})_{0.53}(Se_{0.08}S)$ on the basis of 1 S, with an empirical formula of RuS_2.
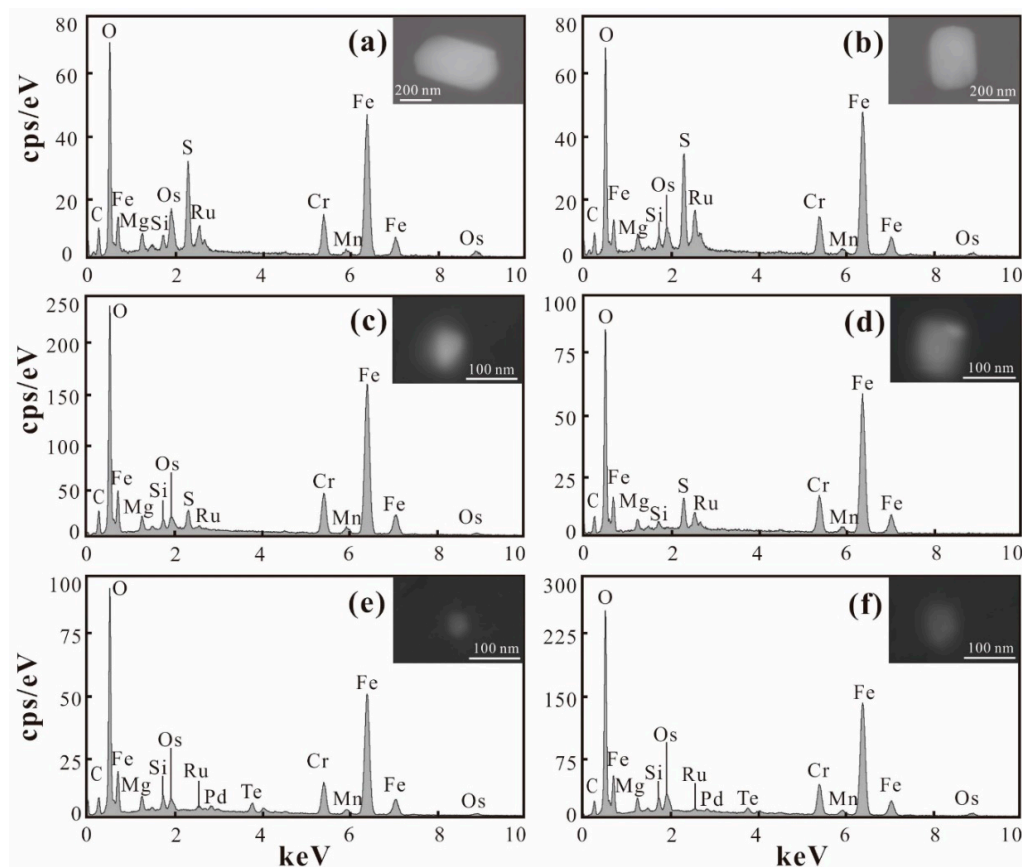
Figure 3. Energy dispersive X-ray spectrometry (EDS) and backscattered electron (BSE) images of platinum-group mineral (PGM) inclusions in chromite in the Xiadong dunites. (**a**–**c**) Ru–Os–S; (**d**) Ru–S; (**e**,**f**) Os–Ru–Pd–Te.
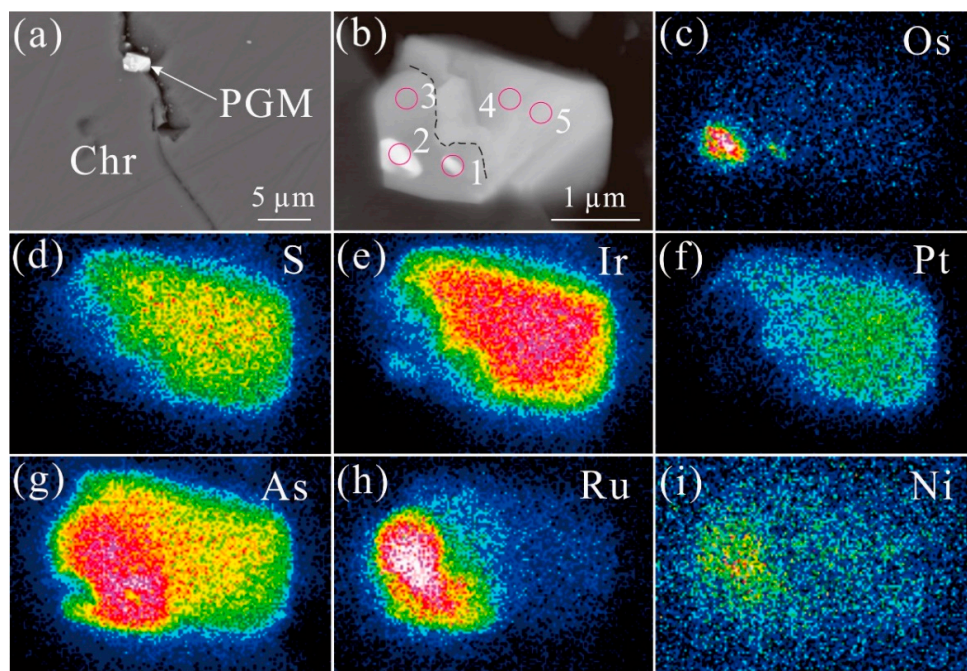

Figure 4. BSE images and S, As, Ir, Ru, Pt, Os, and Ni element maps of a three-phas PGM grain from the chromite fracture. (**a**,**b**) BSE images; (**c**–**i**) Os, S, Ir, Pt, As, Ru, and Ni element maps. Chr: chromite; numbers represent-the positions of semi-quantitative spot analyses listed in Table 1.
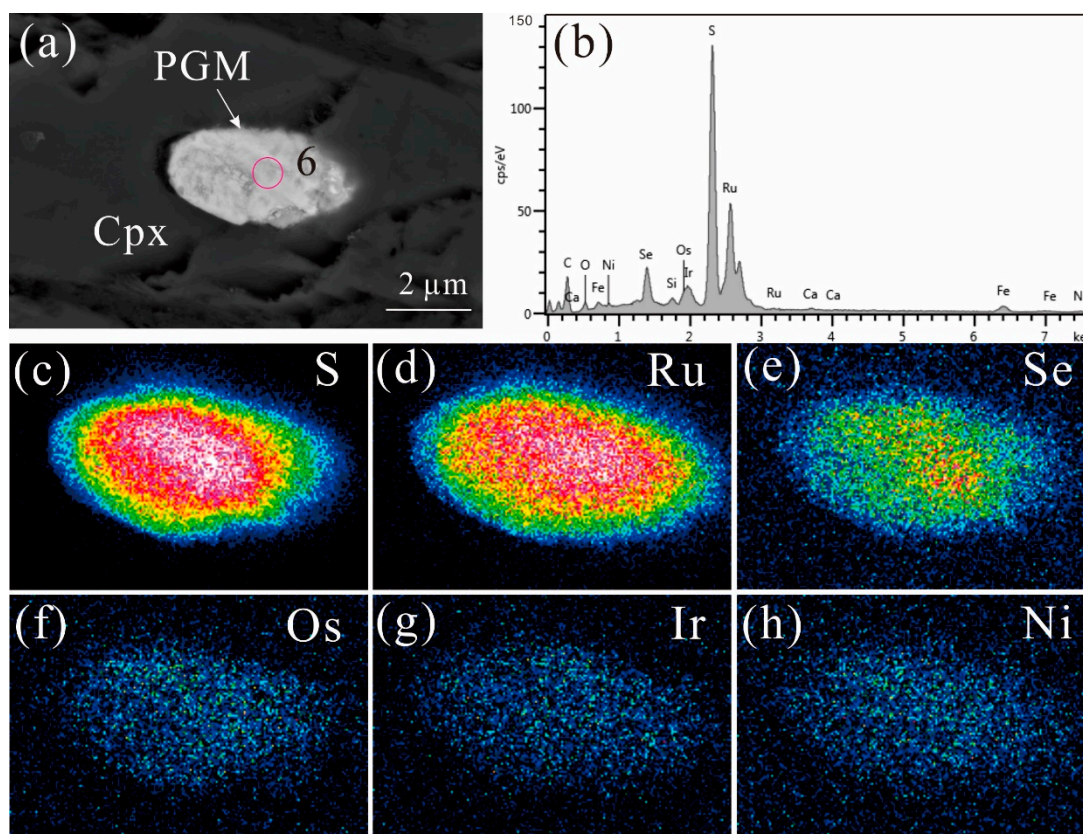
Figure 5. BSE images and S, Ru, Se, Os, Ir, and Ni element maps of a single phase of PGM grain from the silicate matrix of clinopyroxene. (**a**) BSE image; (**b**) the EDS spectrum of spot 6; (**c–h**) S, Ru, Se, Os, Ir, and Ni element maps. Cpx: clinopyroxene; 6: the position of semi-quantitative spot analysis of spot 6 in Table 1.

A variety of sulfides and sulfarsenide occur as inclusions within chromite (Figure 6) and serpentinized olivine (Figure 7), as well as in fractures of chromite (Figure 6). Chemically, they are maucherite ($Ni_{11}As_8$), pentlandite (($Fe,Ni)_9S_8$), millerite (NiS), heazlewoodite (Ni_3S_2), jaipurite (CoS), and galena (PbS). The largest grain size was 10 μm. Maucherite enclosed in chromite was mostly associated with heazlewoodite (Figure 6b,c), whereas those in the serpentinized olivine mostly occurred as single mineral phases (Figure 7a), occasionally associated with pentlandite (Figure 7b). Pentlandite phases also mainly occurred as single grains (Figure 6i–l) and were sometimes associated with galena in chromite (Figure 6g,h), and maucherite in serpentinized olivine (Figure 7b,d).
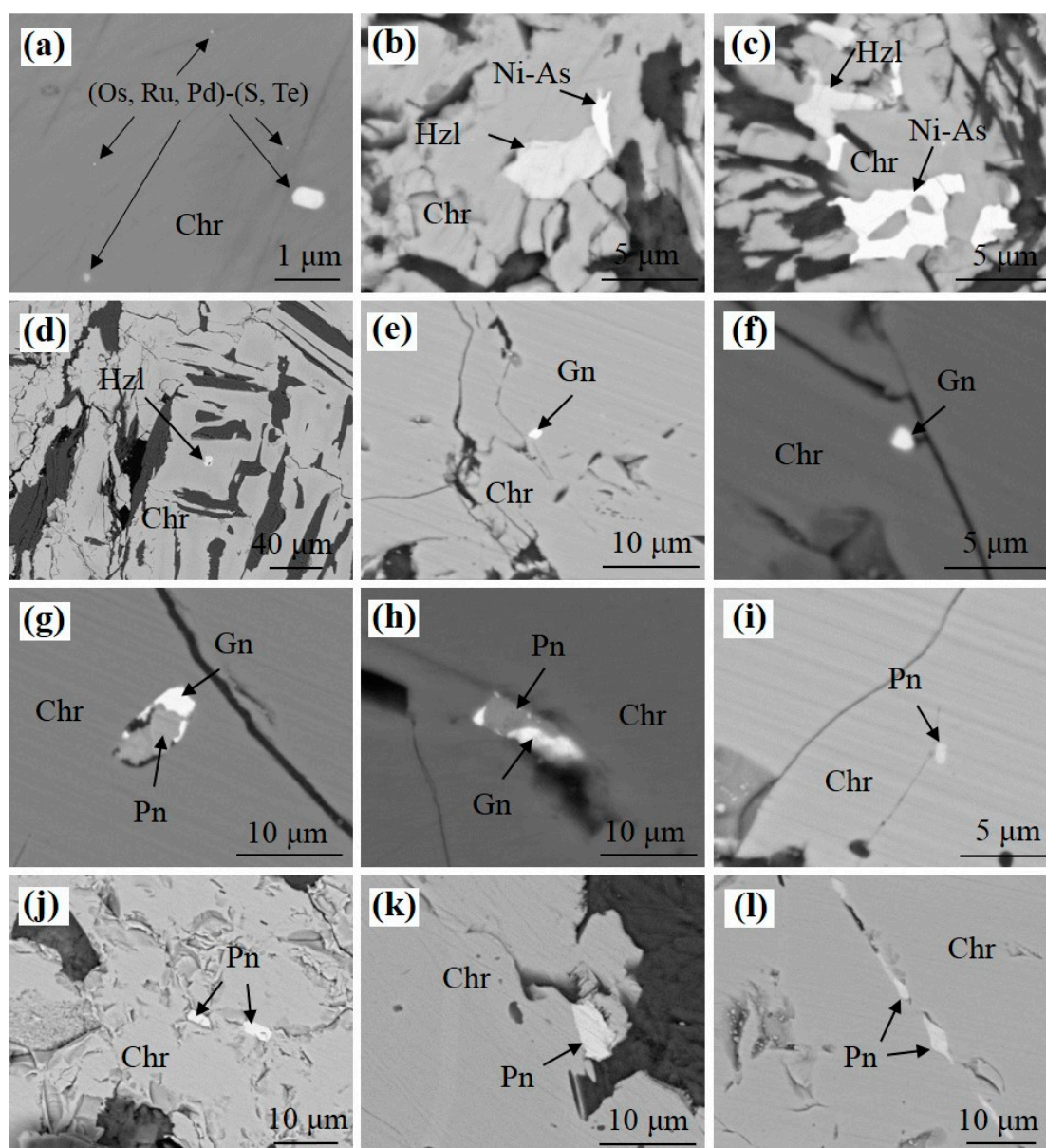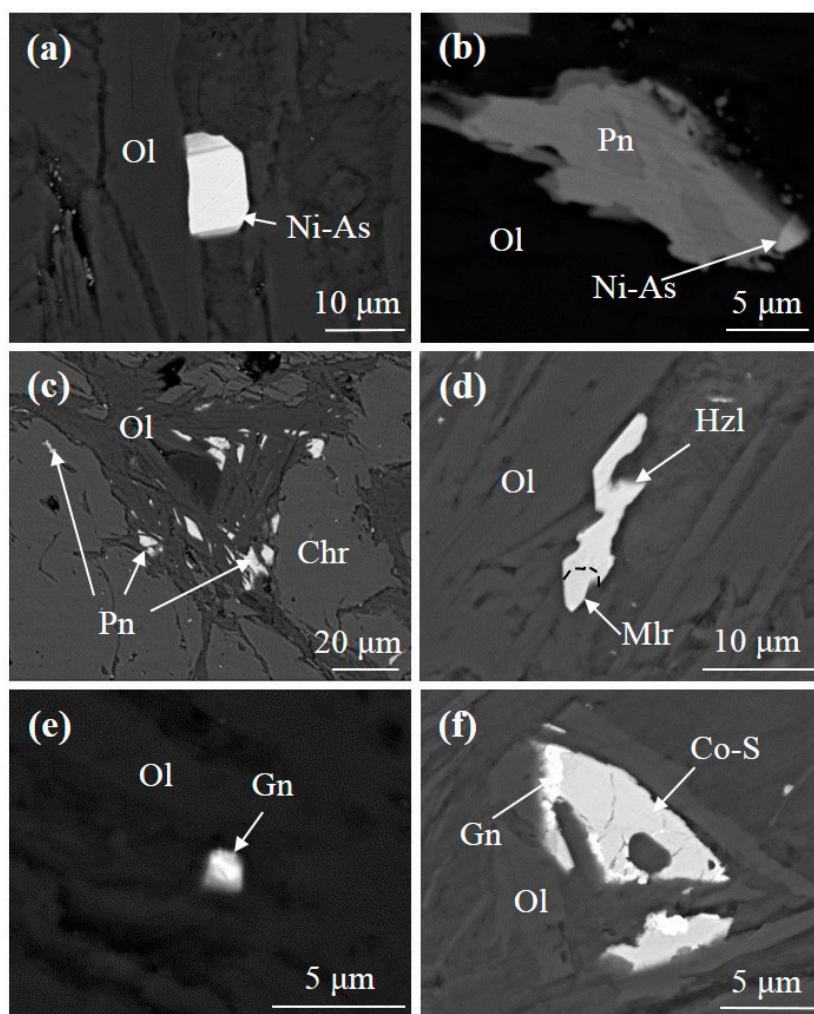
Figure 6. BSE images of base-metal minerals in chromite. (**a**) PGM of Os–Ru–Pd–S–Te; (**b,c**) heazlewoodite associated with maucherite; (**d**) heazlewoodite occurring as a single mineral phase; (**e,f**) galena occurring as a single mineral phase; (**g,h**) pentlandites associated with galena; (**i–l**) pentlandites occurring as a single mineral phase. Ni–As: maucherite; Hzl: heazlewoodite; Gn: galena; Pn: pentlandite.

Table 1. Representative energy dispersive spectrometry (EDS) analyses of platinum-group minerals from the Xiadong Alaskan-type complex.

Element/ Spot	Os	Ir	Ru	Pt	Fe	Ni	Se	As	S	Total (wt.%)	Os *	Ir *	Ru *	Pt *	Fe *	Ni *	Se *	As *	S *
1	52.9	11.6	34.5	-	-	1.0	-	-	-	100	0.40	0.09	0.49	-	-	0.03	-	-	-
2	54.2	11.3	34.5	-	-	-	-	-	-	100	0.42	0.09	0.50	-	-	-	-	-	-
3	-	18.9	32.9	5.50	-	2.20	-	37.1	3.50	100	-	0.91	3.01	0.26	-	0.34	-	4.58	1.00
4	-	60.6	3.10	-	-	-	-	23.3	13.1	100	-	0.77	0.08	-	-	-	-	0.76	1.00
5	-	60.0	3.40	-	-	-	-	23.4	13.1	100	-	0.77	0.08	-	-	-	-	0.77	1.00
6	5.60	5.30	44.2	-	4.70	0.90	5.70	-	33.6	100	0.03	0.03	0.47	-	0.09	0.02	0.08	-	1.00

Note: 1 and 2—Os–Ir–Ru alloys; 3—$(Ru, Ir, Pt, Ni)_{0.81}(As_{4.58}S)$; 4 and 5—irarsite; 6—laurite. Element (wt.%); element * (number of atoms).

Figure 7. BSE images of base-metal minerals in serpentinized olivine. (**a**) Euhedral maucherite occurring as a single mineral phase; (**b**) pentlandites associated with maucherite; (**c**) pentlandites occurring as a single mineral phase; (**d**) heazlewoodite associated with millerite; (**e**) galena occurring as a single mineral phase; (**f**) galena occurring at the boundary of jaipurite. Ol: olivine; Mlr: millerite; Co–S: cobaltous sulfide.

4.2. Whole-Rock PGE Geochemistry

The PGE concentrations in dunite, hornblende clinopyroxenite, hornblendite, and hornblende gabbro from the Xiadong complex are reported in Table 2. These rocks show a wide range in total PGE concentrations from 8.69 to 112 ppb for dunite, 3.41 ppb for hornblende clinopyroxenite, 0.38 to 2.08 ppb for hornblendite, and 0.41 to 6.98 ppb for hornblende gabbro.

Irridium concentrations in the dunites varied between 0.80 and 5.02 ppb, whilst the other rock types had relatively low Ir concentrations (<0.1 ppb). Ruthenium concentrations of the dunites varied between 3.27 and 11.0 ppb, which was higher than those of the hornblende clinopyroxenite (2.64 ppb), hornblendites (0.03 to 0.05 ppb), and hornblende gabbros (0.04 to 0.61 ppb). Rhodium concentrations of the dunites varied between 0.63 and 3.34 ppb, whilst the other rock types had lower Rh concentrations (<0.2 ppb). The dunites had a large variation and overall higher Pt concentrations of 0.92 to 50.4 ppb than hornblende clinopyroxenite (0.32 ppb), hornblendite (0.20 to 1.63 ppb), and hornblende gabbro (0.23 to 5.89 ppb). Palladium concentrations in the dunites showed large variation from 0.16 to 42.2 ppb, whilst the other rocks showed limited Pd variations (hornblende clinopyroxenite: 0.23 ppb; hornblendite: 0.12 to 0.38 ppb; hornblende gabbro: 0.10 to 0.47 ppb).

Table 2. Platinum-group element (PGE) concentrations (ppb, except where specified) of the rocks from the Xiadong Alaskan-type complex. PPGE—Pd–PGE; IPGE—Ir–PGE.

Sample	Rock Type	Ir	Ru	Rh	Pt	Pd	Cu (ppm)	∑PGE	IPGE	PPGE	PPGE/IPGE	Pd/Ir	Cu/Pd ($\times 10^3$)
09XDTC1-35	Dunite	5.02	11.0	3.34	50.4	42.2	-	112	16.0	95.9	5.98	8.40	-
09XDTC1-36	Dunite	0.80	4.23	2.02	14.6	12.0	3.37	33.6	5.03	28.6	5.68	15.00	0.28
09XDTC1-15	Dunite	1.28	5.00	0.71	1.49	0.39	246	8.87	6.28	2.59	0.41	0.31	627
09XDTC1-28	Dunite	1.54	3.27	0.75	2.05	1.09	4.73	8.69	4.81	3.88	0.81	0.70	4.35
09XDTC1-29	Dunite	2.61	7.87	0.63	2.09	0.71	-	13.9	10.5	3.44	0.33	0.27	-
09XDTC1-24	Dunite	1.76	5.55	0.78	1.27	0.16	-	9.52	7.31	2.21	0.30	0.09	-
09XDTC1-25	Dunite	1.12	4.82	0.79	2.09	2.80	7.32	11.6	5.95	5.68	0.96	2.49	2.61
09XDTC1-32	Dunite	1.38	5.38	0.79	0.92	1.31	8.35	9.78	6.76	3.02	0.45	0.95	6.38
09XDTC1-10	Hornblende clinopyroxenite	0.07	2.64	0.14	0.32	0.23	9.63	3.41	2.71	0.69	0.26	3.17	41.7
09XDTC1-21	Hornblendite	0.01	0.05	0.04	1.63	0.34	8.91	2.08	0.06	2.02	32.3	26.5	26.2
09XDTC1-37	Hornblendite	0.02	0.05	0.01	0.24	0.38	8.54	0.70	0.07	0.64	9.75	23.4	22.4
09XDTC1-44	Hornblendite	0.01	0.03	0.01	0.20	0.12	7.31	0.38	0.04	0.33	7.50	11.9	59.1
09XDTC1-8	Hornblende gabbro	0.01	0.04	0.01	0.23	0.24	15.0	0.54	0.05	0.49	9.36	19.0	61.5
09XDTC1-12	Hornblende gabbro	0.02	0.05	0.01	0.23	0.10	88.8	0.41	0.07	0.34	4.94	6.61	890
09XDTC1-22	Hornblende gabbro	0.01	0.05	0.03	1.07	0.47	67.2	1.63	0.06	1.57	26.4	41.9	143
XDE2	Hornblende gabbro	0.09	0.61	0.19	5.89	0.20	1.81	6.98	0.70	6.28	9.01	2.27	9.00

5. Discussion

5.1. Primary and Late-Stage Generation of PGM and Sulfide

The PGMs in the Xiadong Alaskan-type complex were mainly PGE sulfides with a few iridium/platinum-group element (IPGE) alloys, PGE sulfarsenides, and tellurides. The inclusion size in chromite was much smaller, usually not exceeding 1 μm, with mainly micro-scale individual grains. Additionally, some inclusions showed euhedral crystals (Figure 3a,b). Some other base metal-minerals including maucherite, pentlandite, millerite, cobaltous sulfide, and galena were also observed. These are different from Alaskan-type complexes found worldwide that are typified by the presence of PGE alloys and the lack of base-metal sulfides [6]. The Pt–Fe alloys, including silicate minerals from Uralian–Alaskan-type intrusion, are formed after the crystallization of chromite, clinopyroxene, and albite. The formation temperature of Pt–Fe alloys is estimated at about 900 °C [5]. In most cases, the inclusions in chromite (Figures 3 and 6), clinopyroxene (Figure 5) and olivine (Figure 7) in the Xiadong Alaskan-type complex were dominated by high-temperature sulfide minerals (e.g., Os–Ru–S, Os–Ru–Pd–Te, Os alloy, and laurite), and would have crystallized from magmas prior to or simultaneously with the formation of the host minerals. A general consensus is that PGMs crystallize prior to or simultaneously with chromite, and deposit from the primary melt in the following order: IPGE alloys, followed by Ru-rich laurite, Os-rich laurite, and finally, base-metal mineral phases [29,30]. The temperature decreases and fS_2 increases [31]. The maximum thermal stability of RuS_2 is experimentally indeed high (1275 °C), consistent with a magmatic crystallization temperature [29]. This crystallization order and the occurrence of high-temperature sulfide minerals suggested for the Xiadong dunites would imply that the PGMs and chromite formed under relatively high fS_2 and temperature conditions. The model for PGE concentration in the Merensky Reef of the Bushveld Complex in South Africa indicates that a silicate melt coexisting with a PGE-enriched sulfide melt with high temperatures of 1200–1400 °C, would be oversaturated by the least soluble PGE upon cooling [32]. With the cooling of a mafic magma, silicate minerals and chromite start crystallizing at some stage and trap some of the PGE "nuggets" [32]. A combined focused ion beam and high-resolution transmission electron microscopy (FIB/HRTEM) investigation of PGE-rich samples from the Merensky Reef suggests that the PGE-rich nanophases found in the base metal sulfide might represent an early phase of magmatic PGM that formed from the silicate melt to be later collected by the sulfide melt [33]. The occurrence of PGE-rich nano inclusions in chromite (Figures 3 and 6) in our study requires that PGMs were already formed in the silicate melt and were subsequently incorporated into the growing chromite grains.

The anduoite–irarsite intergrowth in the cracks of chromite (Figure 4) could be related to late-stage hydrothermal alteration [18]. The incompatible As could have accumulated along with the late-stage PGE sulfides deposited as interstitial phases in the chromitite at a postmagmatic hydrothermal stage of crystallization [34]. Augé et al. [35] affirmed that hydrothermal laurite typically has more As content (1.01–5.97 wt.%) than magmatic laurite. The unidentified phase $(Ru, Ir, Pt, Ni)_{0.81}(As_{4.58}S)$, as well as the occurrence of irarsite, at the margins of PGM grains (Figure 4) indicates the interaction of PGMs with late-stage As- and S-rich fluids. In addition, the laurite in the Xiadong dunite had significantly lower IrS_2 content (<5.3 mol.%; Table 1) than that in ophiolitic chromitite (ca. 15 mol.%) [36], suggesting the limited solubility of Ir in RuS_2. The laurite in clinopyroxene (Figure 5) likely reflects a process of ultimate S loss and Se incorporation into RuS_2 during a late-stage evolution of the H_2O-bearing fluid [37]. Laurite is normally depleted in Se with hundreds of ppm of Se [38].

Heazlewoodite crystallizes under a wide range of T and fS_2 conditions [39]. However, primary heazlewoodite inclusions within the chromite grains (Figure 6b–d) indicate a magmatic origin. Furthermore, the inclusion relationship texturally suggests that the heazlewoodite crystallized prior to or simultaneously with the chromite crystals. Some of the base-metal minerals such as millerite, pentlandite, and galena in the cracks of chromite (Figure 6) or serpentinized olivine (Figure 7) are medium- or low-temperature minerals, and are known to form in hydrothermal systems.

5.2. Relationship between PGM Occurrences and Bulk PGE Concentrations

The rocks of the Xiadong complex displayed large variation in PGE concentration with ∑PGE of 0.38–112 ppb, which is slightly lower than that of Ural–Alaskan-type complexes with ∑PGE of 9.1–196.1 ppb [40]. The highest PGE concentration in the dunite was 112 ppb, indicating PGE enrichment in the parental magma of the Xiadong complex. The dunite samples displayed primitive mantle-normalized PGE patterns with a weakly positive slope from Ir to Pd [41] (Figure 8). It is noteworthy that six dunite samples showed negative slopes from Rh to Pt and had a large variationin Pd (Figure 8). The PGE patterns ranged from nearly unfractionated in the dunites (Pd/Ir = 0.09–15) to mildly fractionated in the hornblende clinopyroxenite, hornblendite, and hornblende gabbro (Pd/Ir = 2.27–41.9). This distinct geochemical behavior was emphasized by the Pd/lr ratio, considered as the "index of fractionation" of the PGE, during petrological processes [40]. Having a chalcophile and siderophile nature, PGEs are mostly concentrated in the earth's core and mantle, but are remarkably low in the crustal "Clarke" values or frequently close to the detection limits [40]. Because of various melting temperatures, PGEs are present in several sulfide phases in the mantle and are incorporated into the melts depending on the degree of partial melting in the mantle [42]. Compared to the mid-ocean range basalt (MORB) PGE concentration with the low degree of partial melting in the range of 2–15% [43], the Xiadong complex showed the higher PGE concentration (Figure 8), suggesting that both IPGEs (Os, Ir, and Ru) and palladium/platinum-group elements (PPGE: Rh, Pt, and Pd) transferred to the melt with high-degree of melting. A higher degree of partial melting can transfer IPGEs from the mantle rocks to the formed melt [44]. On the other hand, a low degree partial melting only transfers PPGEs to the formed melt due to the varying sulfide melt/silicate liquid partition coefficients [45,46]. Quantitative simulation studies indicated that the primitive magma of the Xiadong complex was derived from 24% bulk partial melting of primitive mantle [47]. Whole-rock high-Mg features indicate that they formed from a depleted mantle source under a high degree of partial melting [17].
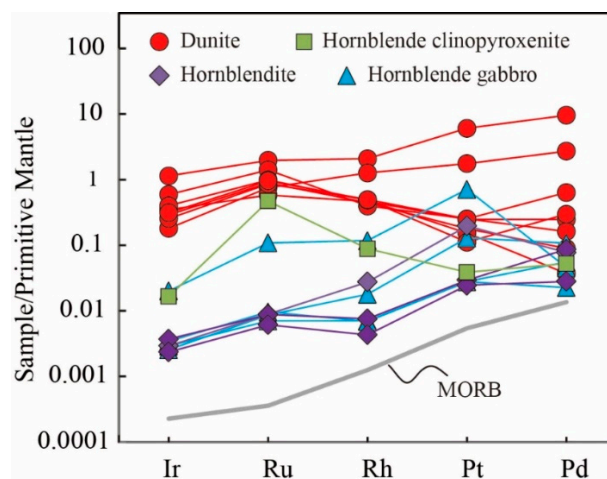
Figure 8. Primitive mantle-normalized PGE patterns for the rocks from the Xiadong Alaskan-type complex. Primitive mantle-normalized values were sourced from Reference [41]. Mid-ocean range basalt (MORB) values were sourced from Reference [43].

Platinum-group elements are commonly found in the form of discrete chromite-hosted PGMs [48]. As discussed above, PGEs are known to be mostly present as micron-sized or nanometer-sized inclusions forming prior to or simultaneously with chromite formation from the silicate magma. Dunite had the highest PGE concentrations (8.69–112 ppb) (Table 2), which is generally consistent with the presence of PGMs. Many laurite and irarsite grains were observed either as euhedral inclusions or along fractures in chromite grains, consistent with IPGE enrichment in all dunites. A few PPGMs were observed with a wide range of concentrations of Pt (0.92 to 50.4) and Pd (0.16 to 42.2) in most dunites (Table 2), suggesting that Pt and Pd were likely to be mobilized during late alteration processes

resulting in differing slopes on the primitive mantle-normalized diagrams (Figure 8). The presence of abundant Pd-bearing PGM is consistent with a pronounced Pd anomaly from chromitites of the Butyrin vein compared with dunite-hosted chromitites at Kytlym, indicating that a high fugacity of sulfur and high-temperature fluids enriched in Hg, Te and Cu play an important roles during the formation of the mineralization in the Butyrin vein [49]. Hornblende clinopyroxenite, hornblendite and hornblende gabbro were all depleted in PGEs, indicating that PGEs were already formed the early solid phases prior to the crystallization of chromite and were mostly collected afterward in dunites during magma differentiation. This is consistent with the identification of only one laurite inclusion in hornblende clinopyroxene (Figure 5).

5.3. Implications on PGE Mineralization in Eastern Tianshan

The formation of PGE-bearing sulfide deposits mainly depends on two conditions: (1) the availability of PGE-rich primary magma and (2) an immiscible sulfide liquid separation and segregation during magma evolution [50]. Palladium and Cu are both considered as incompatible elements with silicate melt [51]. The Pd minimum partition coefficient of 17,000 in sulfide/silicate liquid is considerably higher than the Cu partition coefficient (1000) in sulfide/silicate [46]. Palladium has a stronger sulfide affinity than Cu when sulfide immiscibility occurs [46]. Cu/Pd ratios would remain constant in basaltic magmas during S-undersaturated fractional crystallization [51]. Therefore, the depletion in Pd relative to Cu can provide an estimation of the percentage of crystal fractionation under sulfide saturated conditions required to deplete the magma in PGEs and other chalcophile elements. The Cu/Pd ratio is an important evaluation parameter of magma evolution, and is widely used in the study of PGE deposits [52]. In magma evolution processes, sulfide separation under saturation would result in the significant depletion of Pd relative to Cu in the residual magma, subsequently giving rise to the observed Cu/Pd ratio. In the Xiadong complex, most dunite samples had Cu/Pd ratios (2815–6377) lower than that of the primary mantle (6364) [52], except for one sample having a significantly higher Cu/Pd ratio (627,000). Along with fractional crystallization, Cu/Pd ratios of clinopyroxenite, hornblendite and gabbro in the range of 9000–142,516 were clearly higher than the primary mantle value, indicating that PGE sulfide separation took place prior to or simultaneously with the formation of the dunite.

The PGEs had similar partition coefficients in both sulfide and silicate melts, with a strong preference for the sulfide melt. The crystallization of PGMs in a PGE-rich primary magma indicates that sulfur saturation occurred during the formation of chromite. In addition, the occurrence of a large number of base metal-sulfides as disseminated accessory grains in all dunites indicates that they formed prior to olivine and chromite crystallization. In the early stage of magma crystallization, enrichment of Ni in the rocks depends on the sulfur fugacity [8,18]. Meanwhile, the crystallization of large amounts of chromite and ilmenite results in the loss of Fe^{2+} in the melt leading to sulfur saturation [50]. The availability of sufficient S, As, Te, and PGEs facilitates the formation of PGE sulfides prior to silicate mineral crystallization. The country rocks of the Xiadong complex are dominated by schists, gneisses and marbles, and their occurrences may reduce the oxygen fugacity of the magmas. It was been demonstrated that an increase in the fO$_2$ in melt results in the increase in the degree of partitioning of Ir, Ru, and Rh into spinel [29]. Accordingly, PGEs would not be soluble and could form PGM under reducing fO$_2$. In addition, the generally small sizes of the Alaskan-type complexes (a few to hundreds of km^2) [53] are preferable for sulfur saturation. The Xiadong complex is relatively smaller than most Alaskan-type complexes worldwide and could, therefore, facilitate sulfur saturation.

The Eastern Tianshan is one of the most important Ni–Cu metallogenic provinces in China [21,54]. Abundant mafic–ultramafic complexes are distributed mainly along deep fractures in the Kangguer–Huangshan ductile shear zone in the Jueluotage Belt in the north of Eastern Tianshan (Figure 1B). They are mostly explored for magmatic Ni–Cu sulfide deposits. The two largest Ni–Cu sulfide deposits of Huangshandong and Tulaergen have very low PGE total concentrations

(<5 ppb) [12,55,56]. The Tudun, Hulu, and Xiangshan Ni–Cu sulfide deposits have total PGE concentrations varying from 0.99 ppb to 2.57 ppb [57], 1.98 ppb to 26.6 ppb [58], and 1.21 ppb to 3.26 ppb [55], respectively. The total PGE concentrations of the Baishiquan [59] and Tianyu [60] Ni-Cu sulfide deposits along the northern margin of the Middle Tianshan terrane are relatively high and close to that of the Xiadong complex (Figure 9). The Luodong and Poyi mafic–ultramafic intrusions in the Beishan terrane have low total PGE concentrations with a maximum of 3.18 ppb and 18.8 ppb, respectively [61,62]. In the Kalatongke Ni–Cu sulfide deposit in the northern margin of the Junggar terrane, the total PGE concentrations vary from 0.23 ppb to 43.6 ppb [63]. The Xiarihamu magmatic Fe–Ni–Cu sulfide deposit is the largest magmatic Ni–Cu deposit ever discovered in an arc setting worldwide and is hosted in a small ultramafic body in the Eastern Kunlun Orogenic Belt of the northern Tibet–Qinghai Plateau in western China. The total concentrations of PGEs in the host rocks of the Xiarihamu deposit vary from 0.09 to 1.45 ppb [64]. When compared with other regional mafic–ultramafic complexes (Figure 9), the total concentrations of PGE in the Xiadong Alaskan-type complex are significantly higher than in other intrusions. Furthermore, PGE mineralization was found in a few Cu–Ni sulfide deposits in Eastern Tianshan [65]. In addition, regional geochemical exploration led to the discovery of PGE anomalies in Middle Tianshan terrane [9], whilst sulfide was also discovered in the Xiadong complex [18]. Therefore, the Xiadong Alaskan-type complex could have potential at least the regional anomalies for PGE as well as Ni sulfide exploration.
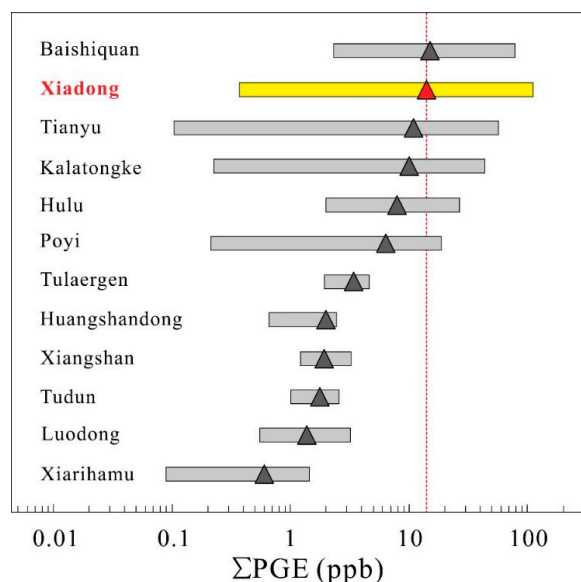
Figure 9. Comparisons of PGE concentrations in the Xiadong Alaskan-type complex and other mafic–ultramafic complexes in the southern Central Asian Orogenic belt (CAOB). Data were taken from References [55–64]. The triangle indicates the average.

6. Conclusions

1. Platinum-group minerals in the dunite from the Xiadong Alaskan-type complex are mainly PGE sulfide and sulfarsenide and occur as inclusions in chromite and clinopyroxene or as interstitial grains along fractures in chromite. The occurrence of PGE-rich inclusions such as laurite in chromite indicates that PGMs already have formed in the silicate melt and subsequently incorporated in the growing chromite grains. The occurrence of interstitial anduoite-irarsite grains along fractures of chromite and Se incorporation in laurite in clinopyroxene are ikely related to late-stage hydrothermal alteration.

2. The dunites have the highest PGE concentrations relative to other lithologies of the Xiadong complex, which is generally consistent with the presence of PGMs. Many laurite and irarsite grains were observed either as euhedral inclusions or along fractures in chromite grains, consistent

with IPGE enrichment in all dunites. A few PPGMs were observed with a wide range of Pt and Pd concentrations in most dunite samples. Hornblende clinopyroxenite, hornblendite and hornblende gabbro are all depleted in PGEs, consistent with the identification of only one laurite inclusion in hornblende clinopyroxene. They also suggest that PGEs had already formed the early solid phases prior to the crystallization of chromite and mostly afterwards were collected in dunites during magma differentiation.

3. Compared to the MORB PGE concentration with the low degree of partial melting, the Xiadong complex shows higher PGE concentration, suggesting that both IPGE and PPGE transferred to the melt with a high-degree of melting. When compared with the regional mafic–ultramafic intrusions in Eastern Tianshan, the Xiadong complex has the greatest PGE enrichment. This is consistent with the identification of PGE anomalies by regional geochemical surveys, demonstrating the potential for PGE mineralization in this region.

References

1. Razin, L.V. Geologic and genetic features of forsterite dunites and their platinum-group mineralization. *Econ. Geol.* **1976**, *71*, 1371–1376. [CrossRef]

2. Cabri, L.J.; Genkin, A.D. Re-examination of Pt alloys from lode and placer deposits, Urals. *Can. Mineral.* **1991**, *29*, 419–425.

3. Barkov, A.Y.; Shvedov, G.I.; Polonyankin, A.A.; Martin, R.F. New and unusual Pd-Tl-bearing mineralization in the Anomal'nyi deposit, Kondyor concentrically zoned complex, northern Khabarovskiy Kray, Russia. *Mineral. Mag.* **2017**, *81*, 679–688. [CrossRef]

4. Johan, Z.; Ohnenstetter, M.; Slansky, E.; Barron, L.M.; Suppel, D. Platinum mineralization in the Alaskan-type intrusive complexes near Fifield, New South Wales, Australia Part 1. Platinum-group minerals in clinopyroxenites of the Kelvin Grove Prospect, owendale intrusion. *Miner. Petrol.* **1989**, *40*, 289–309. [CrossRef]

5. Nixon, G.T.; Cabri, L.J.; Laflamme, J.G. Platinum-group element mineralization in lode and placer deposits associated with the Tulameen Alaskan-type complex, British Columbia. *Can. Mineral.* **1990**, *28*, 503–535.

6. Zaccarini, F.; Singh, K.A.; Garuti, G.; Zsatyanarayanan, M. Platinum-group minerals (PGM) in the chromitite from the Nuasahi massif, eastern India: Further findings and implications for their origin. *Eur. J. Mineral.* **2017**, *29*, 571–584. [CrossRef]

7. Johan, Z. Platinum-group minerals from placers related to the Nizhni Tagil (Middle Urals, Russia) Uralian-Alaskan-type ultramafic complex: Ore-mineralogy and study of silicate inclusions in (Pt, Fe) alloys. *Miner. Petrol.* **2006**, *87*, 1–30. [CrossRef]

8. Johan, Z. Alaskan-type complexes and their platinum-group element mineralization. *Geol. Geochem. Mineral. Miner. Benef. Platin.-Group Elem.* **2002**, *54*, 669–719.

9. Clark, T. Petrology of the Turnagain ultramafic complex, northwestern British Columbia. *Can. J. Earth Sci.* **1980**, *17*, 744–757. [CrossRef]

10. Li, C.; Ripley, E.M.; Thakurta, J.; Stifter, E.C.; Qi, L. Variations of olivine Fo–Ni concentrations and highly chalcophile element abundances in arc ultramafic cumulates, southern Alaska. *Chem. Geol.* **2013**, *351*, 15–28. [CrossRef]

11. Zhang, H.; Liu, H.Y.; Chen, F.L. Regional geochemical exploration for platinum and palladium. *Geochimica* **2002**, *31*, 55–65. (In Chinese with English abstract)

12. Qin, K.Z.; Su, B.X.; Sakyi, P.A.; Tang, D.M.; Li, X.H.; Sun, H.; Liu, P.P. SIMS zircon U-Pb geochronology and Sr-Nd isotopes of Ni-Cu-bearing mafic-ultramafic intrusions in Eastern Tianshan and Beishan in correlation with flood basalts in Tarim Basin (NW China): Constraints on a ca. 280 Ma mantle plume. *Am. J. Sci.* **2011**, *311*, 237–260. [CrossRef]

13. Su, B.X.; Qin, K.Z.; Sakyi, P.A.; Li, X.H.; Yang, Y.H.; Sun, H.; Tang, D.M.; Liu, P.P.; Xiao, Q.H.; Malaviarachchi, S.P.K. U-Pb ages and Hf-O isotopes of zircons from Late Paleozoic mafic-ultramafic units in southern Central Asian Orogenic Belt: Tectonic implications and evidence for an Early-Permian mantle plume. *Gondwana Res.* **2011**, *20*, 516–531. [CrossRef]

14. Su, B.X.; Qin, K.Z.; Tang, D.M.; Sakyi, P.A.; Liu, P.P.; Sun, H.; Xiao, Q.H. Late Paleozoic mafic-ultramafic intrusions in southern Central Asian Orogenic Belt (NW China): Insight into magmatic Ni-Cu sulfide mineralization in orogenic setting. *Ore Geol. Rev.* **2013**, *51*, 57–73. [CrossRef]

15. Su, B.X.; Qin, K.Z.; Sakyi, P.A.; Malaviarachchi, S.P.K.; Liu, P.P.; Tang, D.M.; Xiao, Q.H.; Sun, H.; Ma, Y.G.; Mao, Q. Occurrence of an Alaskan-type complex in the Middle Tianshan Massif, Central Asian Orogenic Belt: Inferences from petrological and mineralogical studies. *Int. Geol. Rev.* **2012**, *54*, 249–269. [CrossRef]

16. Su, B.X.; Qin, K.Z.; Sun, H.; Tang, D.M.; Xiao, Q.H.; Liu, P.P.; Sakyi, P.A. Olivine compositional mapping of mafic-ultramafic complexes in Eastern Xinjiang (NW China): Implications for mineralization and tectonic dynamics. *J. Earth Sci.* **2012**, *23*, 41–53. [CrossRef]

17. Su, B.X.; Qin, K.Z.; Zhou, M.F.; Sakyi, P.A.; Thakurta, J.; Tang, D.M.; Liu, P.P.; Xiao, Q.H.; Sun, H. Petrological, geochemical and geochronological constraints on the origin of the Xiadong Ural-Alaskan type complex in NW China and tectonic implication for the evolution of southern Central Asian Orogenic Belt. *Lithos* **2014**, *200*, 226–240. [CrossRef]

18. Bai, Y.; Su, B.X.; Chen, C.; Yang, S.H.; Liang, Z.; Xiao, Y.; Qin, K.Z.; Malaviarachchi, S.P.K. Base metal mineral segregation and Fe-Mg exchange inducing extreme compositions of olivine and chromite from the Xiadong Alaskan-type complex in the southern part of the Central Asian Orogenic Belt. *Ore Geol. Rev.* **2017**, *90*, 184–192. [CrossRef]

19. Su, B.X.; Hu, Y.; Teng, F.Z.; Qin, K.Z.; Bai, Y.; Sakyi, P.A.; Tang, D.M. Chromite-induced magnesium isotope fractionation during mafic magma differentiation. *Sci. Bull.* **2017**, *62*, 1538–1546. [CrossRef]

20. Su, B.X.; Chen, C.; Bai, Y.; Pang, K.N.; Qin, K.Z.; Sakyi, P.A. Lithium isotopic composition of Alaskan-type intrusion and its implication. *Lithos* **2017**, *286–287*, 363–368. [CrossRef]

21. Qin, K.Z.; Zhang, L.C.; Xiao, W.J.; Xu, X.W.; Yan, Z.; Mao, J.W. Overview of major Au, Cu, Ni and Fe deposits and metallogenic evolution of the eastern Tianshan Mountains, Northwestern China. *Tecton. Evol. Metall. Chin. Altay Tianshan* **2003**, *10*, 227–248.

22. Zhang, M.J.; Li, C.S.; Fu, P.E.; Hu, P.Q.; Ripley, E.M. The Permian Huangshanxi Cu-Ni deposit in western China: Intrusive-extrusive association, ore genesis and exploration implications. *Miner. Depos.* **2011**, *46*, 153–170. [CrossRef]

23. Xie, X.J. Global geochemical mapping. *Geol. China* **2003**, *30*, 1–9. (In Chinese with English abstract)

24. Tang, D.M.; Qin, K.Z.; Sun, H.; Su, B.X.; Xiao, Q.H. The role of crustal contamination in the formation of Ni-Cu sulfide deposits in Eastern Tianshan, Xinjiang, Northwest China: Evidence from trace element geochemistry, Re-Os, Sr-Nd, zircon Hf-O, and sulfur isotopes. *J. Asian Earth Sci.* **2012**, *49*, 145–160. [CrossRef]

25. Qi, L.; Jing, H.; Gregoire, D.C. Determination of trace elements in granites by inductively coupled plasma mass spectrometry. *Talanta* **2000**, *51*, 507–513.

26. Qi, L.; Gao, J.; Huang, X.; Hu, J.; Zhou, M.F.; Zhong, H. An improved digestion technique for determination of platinum group elements in geological samples. *J. Anal. Atom. Spectrom.* **2011**, *26*, 1900–1904. [CrossRef]

27. Qi, L.; Zhou, M.F.; Wang, C.Y. Determination of low concentrations of platinum group elements in geological samples by ID-ICP-MS. *J. Anal. Atom. Spectrom.* **2004**, *19*, 1335–1339. [CrossRef]

28. Yu, T.; Chou, H. Anduoite, a new ruthenium arsenide. *Chinese Sci. Bull.* **1979**, *15*, 704–708. (In Chinese with English abstract)

29. Brenan, J.M.; Andrews, D.R.A. High–temperature stability of laurite and Ru Os–Ir alloys and their role in PGE fractionation in mafic magmas. *Can. Mineral.* **2001**, *39*, 341–360. [CrossRef]

30. Garuti, G.; Zaccarini, F.; Proenza, J.A.; Thalhammer, O.A.; Angeli, N. Platinum-group minerals in chromitites of the Niquelândia layered intrusion (Central Goias, Brazil): Their magmatic origin and low-temperature reworking during serpentinization and lateritic weathering. *Minerals* **2012**, *2*, 365–384. [CrossRef]

31. Uysal, İ.; Akmaz, R.M.; Kapsiotis, A.; Demir, Y.; Saka, S.; Avcı, E.; Müller, D. Genesis and geodynamic significance of chromitites from the Orhaneli and Harmancık ophiolites (Bursa, NW Turkey) as evidenced by mineralogical and compositional data. *Ore Geol. Rev.* **2015**, *65*, 26–41. [CrossRef]

32. Ballhaus, C.; Sylvester, P. Noble metal enrichment processes in the Merensky Reef, Bushveld Complex. *J. Petrol.* **2000**, *41*, 545–561. [CrossRef]

33. Wirth, R.; Reid, D.; Schreiber, A. Nanometer-sized platinum-group minerals (PGM) in base metal sulfides: New evidence for an orthomagmatic origin of the Merensky Reef PGE ore deposit, Bushveld Complex, South Africa. *Can. Mineral.* **2013**, *51*, 143–155. [CrossRef]

34. Barkov, A.Y.; Fleet, M.E. An unusual association of hydrothermal platinum-group minerals from the Imandra layered complex, Kola Peninsula, northwestern Russia. *Can. Mineral.* **2004**, *42*, 455–467. [CrossRef]

35. Augé, T.; Genna, A.; Legendre, Q.; Ivanov, K.S.; Volchenko, Y.A. Primary platinum mineralization in the Nizhny Tagil and Kachkanar ultramafic complexes, Urals, Russia: A genetic model for PGE concentration in chromite-rich zones. *Econ. Geol.* **2005**, *100*, 707–732. [CrossRef]

36. Cabri, L.J. The geology, geochemistry, mineralogy and mineral beneficiation of platinum-group elements. *Can. Inst. Min. Metall. Pet.* **2002**, *54*, 13–129.

37. Barkov, A.Y.; Nikiforov, A.A.; Tolstykh, N.D.; Shvedov, G.I.; Korolyuk, V.N. Compounds of Ru-Se-S, alloys of Os-Ir, framboidal Ru nanophases and laurite-clinochlore intergrowths in the Pados-Tundra complex, Kola Peninsula, Russia. *Eur. J. Mineral.* **2017**, *29*, 613–622. [CrossRef]

38. Hattori, K.H.; Cabri, L.J.; Johanson, B.; Zientek, M.L. Origin of placer laurite from Borneo: Se and As contents, and S isotopic compositions. *Mineral. Mag.* **2004**, *68*, 353–368. [CrossRef]

39. Stockman, H.W.; Hlava, P.F. Platinum–group minerals in alpine chromitites from Southwestern Oregon. *Econ. Geol.* **1984**, *79*, 491–508. [CrossRef]

40. Garuti, G.; Fershtater, G.B.; Bea, F.; Montero, P.; Pushkarev, E.; Zaccarini, F. Platinum-group elements as petrological indicators in mafic-ultramafic complexes of the central and southern Urals. *Tectonophysics* **1997**, *276*, 181–194. [CrossRef]

41. González-Jiménez, J.M.; Proenza, J.A.; Gervilla, F.; Melgarejo, J.C.; Blanco-Moreno, J.A.; Ruiz-Sanchez, R.; Griffin, W.L. High-Cr and high-Al chromitites from the Sagua de Tanamo District, Mayari-Cristal ophiolitic massif (Eastern Cuba): Constraints on their origin from mineralogy and geochemistry of chromian spinel and platinum group elements. *Lithos* **2011**, *125*, 101–121. [CrossRef]

42. Barnes, S.J.; Boyd, R.; Korneliusson, A.; Nilsson, L.P.; Often, M.; Pedersen, R.B.; Robins, B. The use of mantle normalization and metal ratios in discriminating between the effects of partial melting, crystal fractionation and sulfide segregation on platinum-group elements, gold, nickel and copper: Examples from Norway. In *Geo-Platinum 87*; Springer: Dordrecht, The Netherlands, 1988; pp. 113–143.

43. Maier, W.D.; Barnes, S.J.; Marsh, J.S. The concentrations of the noble metals in southern African flood-type basalts and MORB: Implications for petrogenesis and magmatic sulphide exploration. *Contrib. Mineral. Pet.* **2003**, *146*, 44–61. [CrossRef]

44. Lorand, J.P.; Alard, O. Platinum-group element abundances in the upper mantle: New constraints from in situ and whole-rock analyses of Massif Central xenoliths (France). *Geochim. Cosmochim. Acta* **2001**, *65*, 2789–2806. [CrossRef]

45. Leblanc, M. Platinum-group glements and gold in Gphiolitic complexes: Distribution and fractionation from mantle to oceanic floor. In *Ophiolite Genesis and Evolution of the Oceanic Lithosphere*; Petters, T.J., Nicolas, A., Coleman, R., Eds.; Springer: Dordrecht, The Netherlands, 1991; pp. 231–260.

46. Fleet, M.E.; Crocket, J.H.; Liu, M.; Stone, W.E. Laboratory partitioning of platinum-group elements (PGE) and gold with application to magmatic sulfide-PGE deposits. *Lithos* **1999**, *47*, 127–142. [CrossRef]

47. Sun, H. Ore-Forming Mechanism in Conduit System and Ore-Bearing Property Evaluation for Mafic-Ultramafic Complex in Eastern Tianshan, Xinjiang. Ph.D. Thesis, Institute of Geology and Geophysics, Chinese Academy of Sciences, Beijing, China, 2009. (In Chinese with English abstract).

48. Kiseleva, O.N.; Zhmodik, S.M.; Damdinov, B.B.; Agafonov, L.V.; Belyanin, D.K. Composition and evolution of PGE mineralization in chromite ores from the Il'chir ophiolite complex (Ospa-Kitoi and Khara-Nur areas, East Sayan). *Russ. Geol. Geophys.* **2014**, *55*, 259–272. [CrossRef]

49. Zaccarini, F.; Garuti, G.; Pushkarev, E.V. Unusually PGE-rich chromitite in the Butyrin vein of the Kytlym Uralian-Alaskan complex, Northern Urals, Russia. *Can. Mineral.* **2011**, *49*, 52–72. [CrossRef]

50. Maier, W.D. Platinum-group element (PGE) deposits and occurrences: Mineralization styles, genetic concepts, and exploration criteria. *J. Afr. Earth Sci.* **2005**, *41*, 165–191. [CrossRef]

51. Song, X.Y.; Li, X.R. Geochemistry of the Kalatongke Ni-Cu-(PGE) sulfide deposit, NW China: Implications for the format ion of magmatic sulfide mineralization in a post collisional environment. *Miner. Depos.* **2009**, *44*, 303–327. [CrossRef]

52. Barnes, S.J.; Picard, C.P. The behaviour of platinum-group elements during partial melting, crystal fractionation, and sulfide segregation: An example from the Cape Smith Fold Belt, northern Quebec. *Geochim. Cosmochim. Acta* **1993**, *57*, 79–87. [CrossRef]

53. Guillou-Frottier, L.; Burov, E.; Augé, T.; Gloaguen, E. Rheological conditions for emplacement of Ural-Alaskan-type ultramafic complexes. *Tectonophysics* **2014**, *631*, 130–145. [CrossRef]

54. Qin, K.Z.; Sun, H.; San, J.Z.; Xu, X.W.; Tang, D.M.; Ding, K.S.; Xiao, Q.H.; Su, B.X. Tectonic setting, geological features and evaluation of ore-bearing property for magmatic Cu-Ni deposits in eastern Tianshan, NW China: Proceedings of Xi'an International Ni-Cu (Pt) Deposit Symposium. *Northwest. Geol.* **2009**, *42*, 95–99.

55. Sun, H.; Qin, K.Z.; Li, J.X.; Tang, D.M.; Fan, X.; Xiao, Q.H. Constraint of mantle partial melting on PGE mineralization of mafic-ultramafic intrusions in Eastern Tianshan: Case study on Tulargen and Xiangshan Cu-Ni deposits. *Acta Petrol. Sin.* **2008**, *24*, 1079–1086. (In Chinese with English abstract) [CrossRef]

56. Qian, Z.Z.; Sun, T.; Tang, Z.L.; Jiang, C.Y.; He, K.; Xia, M.Z.; Wang, J.Z. Platinum-group elements geochemistry and its significances of the Huangshandong Ni-Cu sulfide deposit, Eastern Tianshan, China. *Geol. Rev.* **2009**, *55*, 874–884. (In Chinese with English abstract)

57. Wang, M.F.; Xia, Q.L.; Xiao, F.; Wang, X.Q.; Yang, W.S.; Jiang, C.L. Rock geochemistry and platinum group elements characteristics of Tudun Cu-Ni sulfide deposit in Eastern Tianshan Mountains of Xinjiang and their metallogenic implications. *Miner. Depos.* **2012**, *31*, 1195–1210. (In Chinese with English abstract)

58. Sun, T.; Qian, Z.Z.; Tang, Z.L.; Jiang, C.Y.; He, K.; Sun, Y.L.; Wang, J.Z.; Xia, M.Z. Zircon U-Pb chronology platinum-group elements geochemistry characteristics of Hulu Cu-Ni deposit, Eastern Xinjiang and its geological significance. *Acta Petrol. Sin.* **2010**, *26*, 3339–3349. (In Chinese with English abstract)

59. Chai, F.M.; Xia, F.; Chen, B.; Lu, H.F.; Wang, H.; Li, J.; Yan, Y.P. Platinum group elements geochemistry of two mafic-ultramafic intrusions in the Beishan block, Xinjiang, NW China. *Acta Geol. Sin.* **2013**, *87*, 474–685. (In Chinese with English abstract)

60. Tang, D.M.; Qin, K.Z.; Sun, H.; Qi, L.; Xiao, Q.H.; Su, B.X. PGE Geochemical characteristics of Tianyu magmatic Cu-Ni deposit: Implications for magma evolution and sulfide segregation. *Acta Geol. Sin.* **2009**, *83*, 680–697. (In Chinese with English abstract)

61. Chai, F.M.; Zhang, Z.C.; Mao, J.W.; Dong, L.H.; Ye, H.S.; Wu, H.; Mo, X.H. Platinum group elements geochemistry of Baishiquan mafic-ultramafic intrusions in Central Tianshan block, Xinjiang. *Acta Geol. Sin.* **2006**, *27*, 123–128. (In Chinese with English abstract)

62. Xue, S.C.; Qin, K.Z.; Li, C.S.; Tang, D.M.; Mao, Y.J.; Qi, L.; Ripley, E.M. Geochronological, petrological, and geochemical constraints on Ni-Cu sulfide mineralization in the Poyi ultramafic-troctolitic intrusion in the northeast rim of the Tarim craton, western China. *Econ. Geol.* **2016**, *111*, 1465–1484. [CrossRef]

63. Qian, Z.Z.; Wang, J.Z.; Jiang, J.G.; Yan, H.Q.; He, K.; Sun, T. Geochemistry characters of platinum group elements and its significations on the process of mineralization in the Kalatongke Cu-Ni sulfide deposit, Xinjiang, China. *Acta Petrol. Sin.* **2009**, *25*, 832–844. (In Chinese with English abstract)

64. Zhang, Z.W.; Tang, Q.Y.; Li, C.S.; Wang, Y.L.; Ripley, E.M. Sr-Nd-Os-S isotope and PGE geochemistry of the Xiarihamu magmatic sulfide deposit in the Qinghai-Tibet plateau, China. *Miner. Depos.* **2016**, *52*, 51–68. [CrossRef]

65. Qin, K.Z.; Tang, D.M.; Su, B.X.; Mao, Y.J.; Xue, S.C.; Tian, Y.; Sun, H.; San, J.Z.; Xiao, Q.H.; Deng, G. The tectonic setting, style, basic feature, relative erosion degree, ore-bearing evaluation sign, potential analysis of mineralization of Cu-Ni-bearing Permian mafic-ultramafic complexes, northern Xinjiang. *Northwest. Geol.* **2012**, *45*, 83–116. (In Chinese with English abstract)